SCIENCE CHINA
Technological Sciences

May 2012 Vol.55 No.5: 1287–1294
doi: 10.1007/s11431-012-4781-1

Plasmaspheric trough evolution under different conditions of subauroral ion drift

HE Fei[1], ZHANG XiaoXin[2*], CHEN Bo[1] & FOK MeiChing[3]

[1] *Changchun Institute of Optics, Fine Mechanics and Physics, Chinese Academy of Sciences, Changchun 130033, China;*
[2] *National Center for Space Weather, China Meteorological Administration, Beijing 100081, China;*
[3] *NASA Goddard Space Flight Center, Greenbelt, MD 20771, USA*

Received January 19, 2012; accepted February 15, 2012; published online March 2, 2012

The statistical characteristics of the subauroral ion drift (SAID) in the ionosphere and the plasmaspheric trough evolution under different conditions of SAID were investigated in this paper, based on 566 SAID events observed by Akebono, Astrid-2, DE-2, and Freja satellites. The relationships between the latitudinal location of SAID and the Kp, AL, and Dst indices for these events were also discussed. It was found that the SAID events happened mainly at invariant latitude (ILAT) of 60.4° and magnetic local time (MLT) of 21.6 MLT and that 92.4% of the events happened when the Kp index was below 5.0, indicating a medium geomagnetic activity. The latitudinal half-width of SAID varied from 0.5° to 3.0° with a typical half-width of 1.0°. The SAID would happen at low latitudes if the geomagnetic activity was high. The effects of SAID on equatorial outer plasmasphere trough evolutions were studied with the dynamic global core plasma model (DGCPM) driven by the statistical results of SAID signatures. It was noted that locations, shapes and density of troughs vary with ILAT, MLT, latitudinal width, cross polar cap potential and lifetime of SAID events. The evolution of a trough is determined by the extent of SAID electric field penetrating into plasmasphere and not all SAID events can result in trough formations.

subauroral ion drift, plasmaspheric trough, dynamic global core plasma model, simulation

Citation: He F, Zhang X X, Chen B, et al. Plasmaspheric trough evolution under different conditions of subauroral ion drift. Sci China Tech Sci, 2012, 55: 1287–1294, doi: 10.1007/s11431-012-4781-1

1 Introduction

The subauroral ion drift (SAID) is a latitudinally narrow region of rapid westward ion drift located in the evening sector on the equatorward edge of the aurora oval in the ionosphere. SAID is a spectacular substorm phenomenon at subauroral latitudes first reported by Galperin et al. [1]. It has a narrow latitudinal extent and is characterized by a westward drift speed in excess of 1 km/s (at times exceeding 5 km/s), by a temperature peak due to collisions between drift particles and neutral atoms, and by an ionospheric density trough. SAIDs have been observed on several satellites by electric field instruments (EFI) and ion drift meters (IDM) in the ionosphere and magnetosphere [2–6].

A number of SAID origin and evolution mechanisms have been generated. Southwood and Wolf [7] have put forward the basic idea of the physical explanation of SAID that predicts the occurrence of intense electric field in the region between the mid-night and evening sector proton inner edge and the low-latitude edge of electron precipitation. These boundaries are smallest in the mid-night sector as a result of a substorm generated enhancement of the cross-tail magnetospheric electric field. In the Southwood and Wolf model, the SAID appears shortly after the sub-

*Corresponding author (email: xxzhang@cma.gov.cn)

storm onset, but observations have suggested that SAID occurs almost during the substorm recovery phase.

Deminov and Shubin [8] proposed that the modification of ionospheric Pedersen conductivity by field-aligned current (FAC) generated the poleward electric field. However, in their model the greatest effects occur during dusk sector which is contrary to observations.

Anderson et al. [3] analyzed the signatures of SAID and concluded that SAID lasts more than 30 min and less than 3 h. The mid-latitude ionospheric trough was presented prior to SAID turn-on and the SAID deepened the trough. They also noted that the latitudinal shape and location of the ion velocity and concentration profiles were consistent with stagnation and poleward transport of plasma from lower latitudes. Shortly later, Anderson et al. [4] proposed a SAID producing mechanism according to the observations. Approximately 10 min after the substorm onset, under the condition of increment of FAC and separation of ions and electrons precipitation boundaries in mid-night sector, poleward electric fields are generated to close the big region 1 and region 2 FAC in the ionosphere. Further, frictional heating leads to a very large plasma depletion in the F-peak and a reduction of the height-integrated Pedersen conductivity in the E-region. Finally, the intense electric fields are produced between the converging equatorial boundaries of the electron and ion precipitation, resulting in the latitudinally narrow spike signature of SAID event. As the substorm recovers, the FACs diminish, but the SAID is maintained by the loss of ionospheric conductivities until Alfvén layer disappears.

In the mechanisms of De Keyser et al. [9] and De Keyser [10], the flow shear exists across the interface of inward moving injected plasma sheet plasma front and the cold plasmapause is responsible for the generation of intense electric fields in the premidnight sector. In their numerical simulation, the westward ion drift peak is greater than 2 km/s, concentrated in a latitudinal region of 1° located near 60° ILAT and about 30 min after substorm onset, which is in accordance with the observations [4]. However, their model is somewhat simple: They have adopted a simple geometry (dipolar magnetic field, etc.) and largely ignored the dynamics of the ionosphere by considering the unloaded electric circuit.

Galperin [11] used ground-based observations in the subauroral ionosphere to analysis the signatures of the SAID events and set up a semi-quantitative model. He proposed a drift-dispersion mechanism for the SAID formation in which the inward displacements of the equipotentials in the evening and premidnight sectors result in the inclination of the equipotentials with respect to the lines B_{eq}=const in the equatorial plane. Although the model approximates the charge accumulation in the magnetosphere and the discharge processes in the conducting ionosphere with an extremely simplified approach and neglects the nonlinearity and the complicated time development, the results are roughly in accordance with observations.

Previous discussions concern the formation and evolution of the SAID events. Ober et al. [12] have embedded the SAID potentials in the dynamic global core plasma model (DGCPM) to show their effects on the trough density profiles in the outer plasmasphere during high magnetic activity. Below, we will first statistically analyze the SAID events observed by four satellites to get the common signatures of the SAID. Then the DGCPM will be used to investigate the trough evolutions under different configurations of SAID potential.

2 SAID observations

SAID events were collected from the following four satellites.

2.1 DE-2

The Dynamics Explorer 2 (DE-2 or DE-B) satellite was launched into a 90° inclination orbit on 31 July 1981, with an initial apogee near 1000 km and an initial perigee below 300 km. A 90° inclination orbit does not process in sidereal time; thus over a lifetime of approximately one and a half years with over 8000 orbits, all local times were sampled in both the northern and southern hemispheres every 6 months. Of primary interest for our study were the data from the ion drift meters (IDM) [13] which provide the bulk ion drift velocity in the plane perpendicular to the satellite track, and the retarding potential analyzer (RPA) [14] which provided the total ion concentration, the ion temperature, and the bulk ion velocity in the direction of satellite motion.

2.2 Akebono

The Akebono spacecraft was launched on 21 February 1989, into an orbit with an initial apogee near 10500 km and a perigee near 274 km and an orbital period of 3.5 h. The vector DC and quasi-static electric field data were acquired from the electric field detector (EFD-P) [15]. The spin axis was directed sunward such that the GSE Z and Y field components could be measured. The GSE X component was inferred from the assumption that $E\times B$=0 (except under adverse conditions on spacecraft location in the geomagnetic field). The data were averaged over the satellite spin period of 8 s with the accuracy estimated to be better than 3 mV/m. The electric fields were projected along magnetic field lines to 120 km altitude using the international geomagnetic reference field (IGRF85), and the $E\times B$ ion drifts in the magnetic north-south and east-west directions were derived.

2.3 Freja

The Freja satellite was launched on 6 October 1992 with an

apogee of 1750 km and a perigee of 600 km. The electric field instrument consists of three probe pairs, extended on wire booms. Two of the probe pairs are extended to 21 m tip to tip and the third pair to 11 m. Most of the time, the two pairs with the longer extension are used. The electric field experiments can be run in a number of different modes, one of which is used for collecting overview data from entire orbits at a sampling rate of 8 Hz. Data collected in this mode were used in this study to build up a database of observations of subauroral electric fields. The double probe electric field instrument is described in detail by Marklund et al. [16].

2.4 Astrid-2

The Astrid-2 satellite was launched in December 1998 into a circular orbit of 1000 km height. A complete coverage of all local time sectors was performed in both hemispheres during the mission lifetime. An integrated electric and magnetic field instrument (EMMA) [17] onboard Astrid-2 provided measurements of the two spin plane components of the electric field and of the full magnetic field vector. The electric field data were obtained from the sampling of the potential of four electric field probes mounted on wire booms in the spin plane. Sampling could be done at 16256 or 2048 samples/s. The data obtained during operation between 11 January 1999 and 24 July 1999 were used in this study.

According to Anderson et al. [4], SAID events will be defined as a latitudinally confined westward drift exceeding 1000 m/s and located equatorward of the auroral zone. We have collected 566 SAID events from the databases of DE-2, Akebono, Freja, and Astrid-2, which formed the basis of the statistical study of SAID in this work. Since the SAID events observed by the four instruments were at different heights, all the events were traced to ionospheric height of 120 km using Tsyganenko magnetic field model [18] for uniformity of the measurements of the parameters of the SAID events.

3 SAID Statistics

Figure 1 shows the SAID events distribution versus ILAT (Figure 1(a)) and MLT (Figure 1(b)). It is shown in Figure 1(a) that the median ILAT of the SAID events is 60.4° with majority (80%) observed between 55° and 66°. The number of events near 60.0° is smaller than that of surrounding and this may be caused by the coverage of the data sets. Figure 1(b) indicates that the median MLT of the SAID events is 21.6 with majority (80%) observed between 1930 and 2330 MLT. Both results are consistent with previous studies [2, 19].

Figure 2 shows a histogram plot of SAID events versus Kp index. It is shown that the SAID events were most probably observed for median Kp values. Approximately 74% of the SAID events were observed when the Kp values were between 3.0 and 5.0, only 8% of the events were observed when Kp index was greater and equal to 6.0 and 18% of the events were observed when Kp index was less than 3.0. The reason why only a small number of events were observed when Kp was greater than 5.0 is that the period when geomagnetic activity was above the level of Kp>5.0

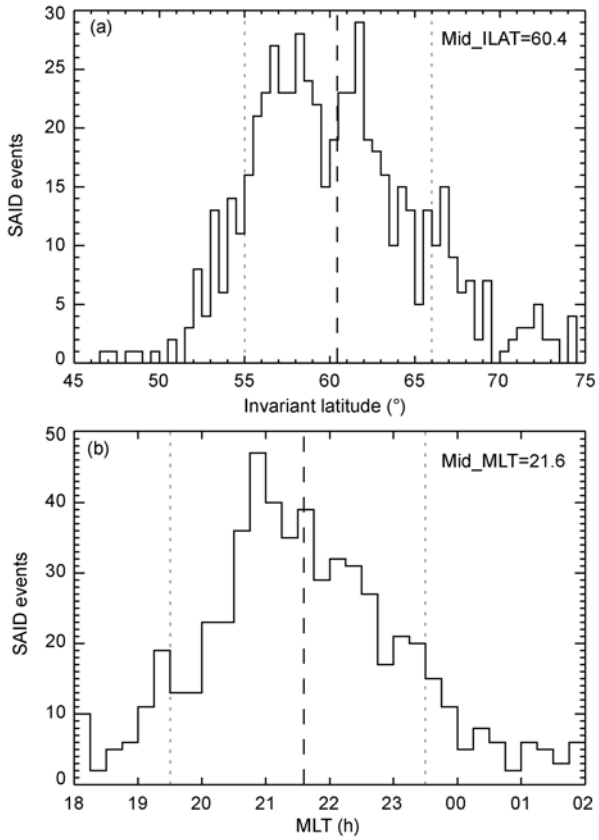

Figure 1 Observed SAID events distribution versus (a) ILAT and (b) MLT. The median values are marked by thick dashed lines. Also shown are the ranges (marked by thin dashed lines) in ILAT and MLT with more than 80% of observed substorms (10% on each side).

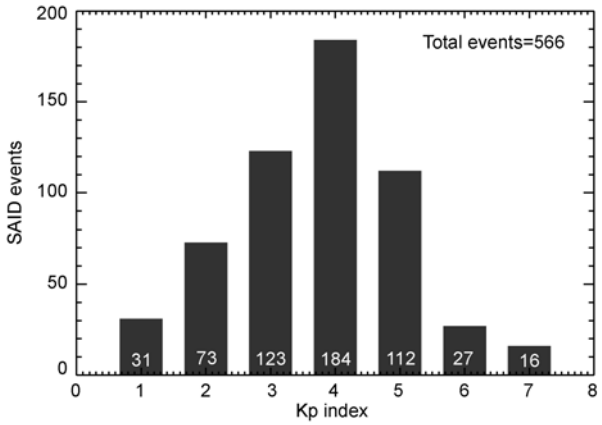

Figure 2 Numbers of SAID events observed with different Kp indexes.

was very short during the time range of the data sets.

The ILAT center of SAID (invariant latitude corresponding to the maximum drift velocity) is least square fitted to the Kp index, as is shown in Figure 3. It is obvious that SAID will move to low latitudes as the Kp index increases. This movement is in accordance with the expansion of auroral oval during high geomagnetic activities. Observations demonstrate that the auroral oval will expand both poleward and equatorward on the nightside with increasing geomagnetic activity [20–22]. The equatorward expansion of auroral oval will push the SAID band to the low latitude. As the auroral oval shrinks during low activity, the SAID band will move to the high latitude. The relationship between the ILAT center of SAID and the Dst index is also presented. Figure 4 shows that ILAT center of SAID increases exponentially with the Dst index. The geomagnetic activity level and the FAC will both affect the latitudinal center of the SAID event. Figure 5 shows that the ILAT center of SAID also decreases exponentially with the AL index, which demonstrates that the particle precipitation and auroral activity will affect the SAID distinctly when the activity is low.

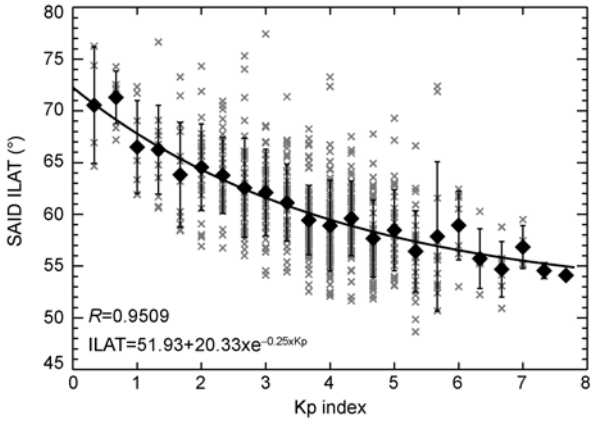

Figure 3 Distribution of ILAT center of SAID versus Kp index. The diamonds represent the averaged ILAT at corresponding Kp value. The solid line represents the least-square fitted relationship between ILAT and Kp index.

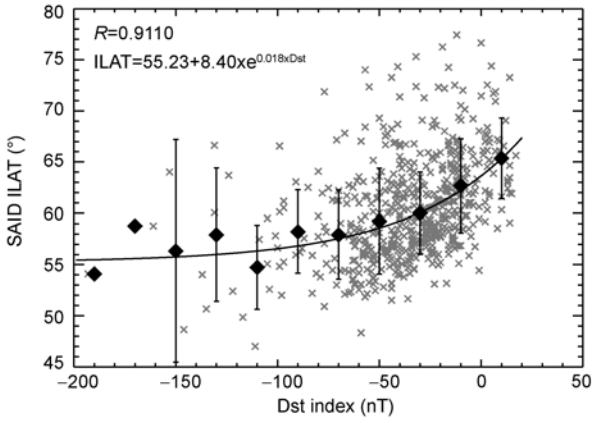

Figure 4 Distribution of ILAT center of SAID versus Dst index. The black diamonds are binned data points with interval of 25 nT. The solid line represents the least-square fitted relationship between ILAT and Dst index.

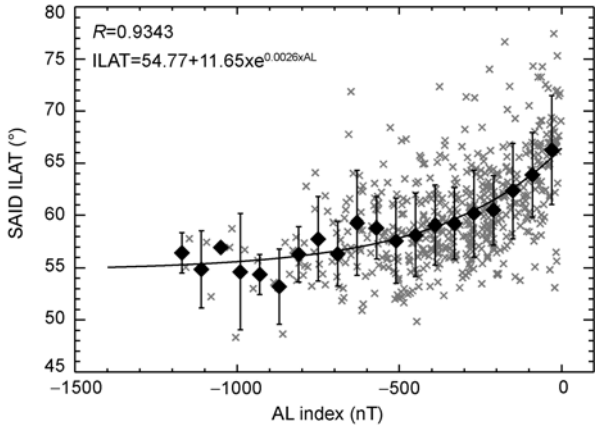

Figure 5 Distribution of ILAT of SAID versus AL index. The black diamonds are binned data points with interval of 50 nT. The solid line represents the least-square fitted relationship between ILAT and AL index.

The relationships in the above three figures reveal that the SAID will move to low latitude as the geomagnetic activity enhances (Kp index increases, Dst index and AL index decrease). According to Anderson et al. [3, 4], SAID events take place during substorms and auroral oval will expand to low latitude during substorms. The stronger the substorm is, the more significant the auroral oval expansion will be. Thus, the above statistics are consistent with the SAID production mechanism of Anderson et al. [4].

The annual variation of the SAID events is present in Figure 6, in which the event numbers are plotted versus day of year (DOY). Most SAID events happening during spring and autumn are consistent with former study [19].

4 SAID effects on plasmasphere trough

The DGCPM [12, 23] is a convection model which calcu-

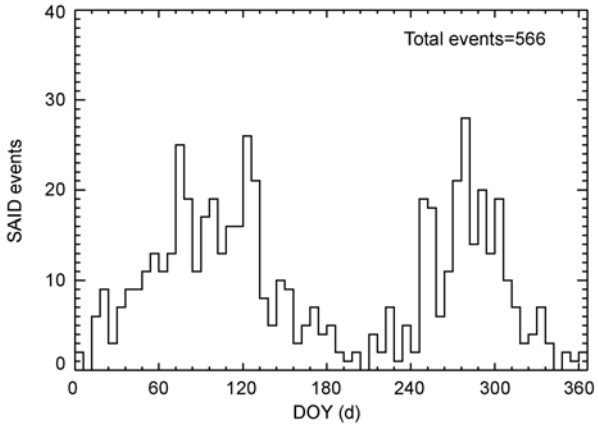

Figure 6 Distribution of the SAID events versus DOY.

lates the cold plasma density in the plasmasphere and surrounding trough regions in the equatorial plane. The ionospheric convection potential model is from Sojka et al. [24], and the SAID potential is the modified Sojka-electric field by Ober [25]. The magnetic field model used in the simulations is T89 [18].

Since SAID events are substorm-related, we embed the SAID potential in our simulation during magnetic storm enhancement of ionospheric convection potential. Anderson et al. [4] have proposed that SAID events most probably occur 30 min or more after the substorm onsets. In all the simulations below, the SAID potentials in the model are all turned on 30 min after the onset of the storm.

It is found that the outer plasmaspheric trough density profiles are related to five signatures of the SAID, the ILAT center (ILATC), latitudinal width (LATW), longitudinal center (LONGC), cross polar cap potential (CPCP) and lifetime (LIFE) of the SAID events. In our model, the SAID potentials do not affect the inner plasmasphere or the plasmasphere boundary layer. According to Horwitz et al. [26] from DE-1 measurements, the trough density profiles were correlated with high Kp, so in the simulations, the ionospheric convection potential is set to be high. In each of the following simulations, the initial density distribution is obtained by two-day convection under quiet activity.

In the following simulations, the typical parameters of SAID are fixed to be 61.0° for ILATC, 1.5° for LATW, 2000 MLT for LONGC, 20 kV for CPCP, and 30 min for LIFE according to above statistics and previous studies [3, 12, 19]. In studying the relationships between plasmaspheric trough and the five signatures of SAID, one signature is variable and the other four are fixed for each simulation. For example, when we investigate the plasmaspheric trough evolution under a different LATW of SAID, the LATW is variable and the other four parameters are fixed to the above values, and so on. The parameter settings for the following five simulations are list in Table 1.

4.1 Trough profiles under different ILATCs of SAID (Simu-A)

Figure 7 shows that different ILATCs of SAID locations have important impact on the equatorial plasmaspheric trough density profiles. According to the statistical analysis in section 3, the ILATC of SAID changes from 58° to 62°. It is clear that as the ILATC increases, the trough becomes deeper and wider; however, the peek density outside the trough decreases. This is because that the magnetic tube volume increases with latitude, and then the density will decrease. The SAID potential almost has no effect on the other parts of the plasmasphere. When the ILATC of SAID is smaller than 59° or greater than 62°, no trough is formed. As the ILATC of SAID moves to high latitude, the inner boundary of trough moves outward slightly. When the ILATC of SAID goes to low latitude adjacent to plasmapause, the SAID electric field penetrates deeply into the plasmasphere and its modulation on the plasmapause is significant. The trough is more apparent when the ILATC of the SAID potential is located near 61°, which is in accordance with satellite observations. On the lower latitude (less than 59.5°) no trough is formed, indicating that the SAID has gone inside the plasmapause and the SAID electric field is shielded by corotation electric field thus having no effect on the plasmapause.

Table 1 Parameter settings for the five simulations

Items	Simu-A	Simu-B	Simu-C	Simu-D	Simu-E
ILATC	variable	61.0°	61.0°	61.0°	61.0°
LATW	1.5°	variable	1.5°	1.5°	1.5°
LONGC	2000 MLT	2000 MLT	variable	2000 MLT	2000 MLT
CPCP	20 kV	20 kV	20 kV	variable	20 kV
LIFE	30 min	30 min	30 min	30 min	variable

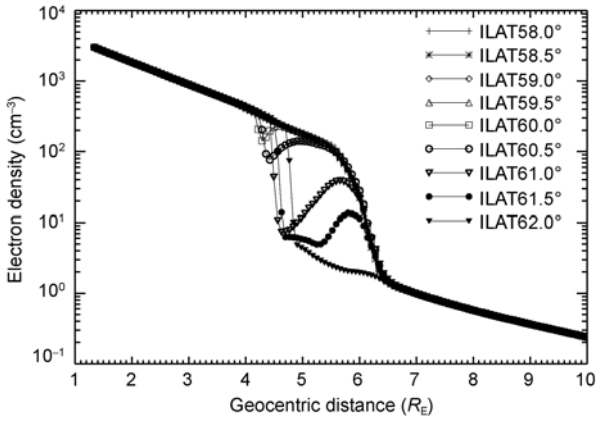

Figure 7 Equatorial plasmaspheric trough density profiles versus geocentric distance under different ILATCs of SAID taken from dusk sector.

4.2 Trough profiles under different LATWs of SAID (Simu-B)

In Figure 8, the trough profiles change with the LATW of SAID. As the width of SAID potential increases, the depth and radial width of trough increase, which means that the density of the radial center of the trough decreases together with the peak density outside the trough. The SAID potential has no effect on the other parts of the plasmasphere either, which can be seen from the superposition of the curves in the figure. The trough is more apparent and typical when the LATW of SAID is between 1.0° and 2.0°, with its peak at the width of 1.5°, which is consistent with satellite observations [3, 4].

4.3 Trough profiles under different LONGCs of SAID (Simu-C)

Figure 9 reveals that the LONGC of SAID potential has

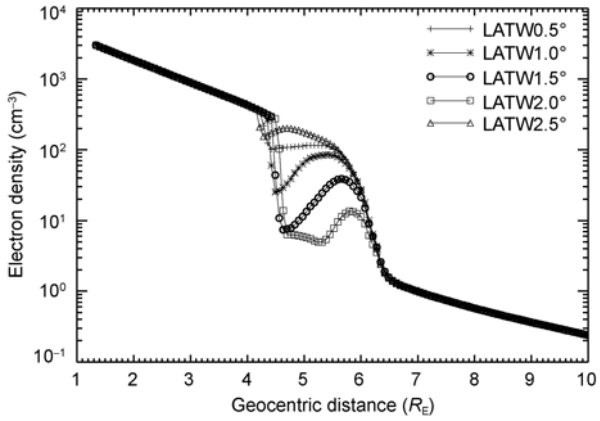

Figure 8 Equatorial plasmaspheric trough density profiles versus geocentric distance under different LATWs of SAID taken from dusk sector.

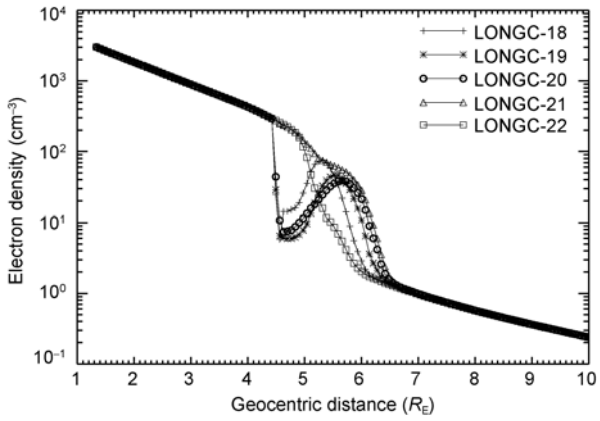

Figure 9 Equatorial plasmaspheric trough density profiles versus geocentric distance under different LONGCs of SAID taken from dusk sector.

little effect on the equatorial plasmaspheric trough density profiles. The inner boundaries of the troughs under different LONGCs have overlapped because the electric field penetrating into the plasmasphere is the same due to the constant ILATC of the SAID. The decrease of peak density may be caused by the change of the shape of the magnetic flux tube, since the magnetic field lines are dragged out by solar wind from noon to midnight, resulting in the increment of the tube volume. When the LONGC is greater than 2200 MLT, no trough appears but the plasmapause still becomes smooth because of partial electric field penetrating.

4.4 Trough profiles under different CPCPs of SAID (Simu-D)

According to satellite observations, the CPCP of SAID ranges from a few to tens of kilovolts [2, 19] and can be greater than 60 kV during large storms [5, 27]. Therefore, the CPCP is limited between 10 and 60 kV in this simulation. Figure 10 shows the trough density profiles versus geocentric distance taken from the dusk sector under different CPCPs of SAID events. It is seen that the CPCP can

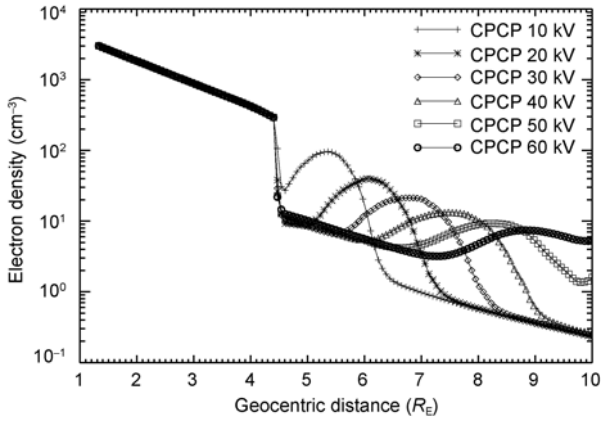

Figure 10 Equatorial plasmaspheric trough density profiles versus geocentric distance under different CPCPs of SAID taken from dusk sector.

significantly change the shapes of troughs. As the CPCP increases, the radial width of trough increases accordingly. This is because that when the potential is high, the corresponding SAID electric field is large and also its latitudinal affecting region, and then its modulating effects on the convection electric field is significant, resulting in a wider radial width of trough.

4.5 Trough profiles under different LIFEs of SAID (Simu-E)

The trough density profiles under different LIFEs of SAID events are also simulated. According to Anderson et al. [3], the lifetime of SAID varies from 30 min to 3 h, mostly turned on after 30 min of substorm onset. In our simulations, we turn on the SAID potentials 30 min after storm enhancement of convection electric field, and the LIFEs considered are 30, 40, 50 and 60 min. It is demonstrated that as the LIFE of SAID potential increases, the trough becomes wider and deeper. This is because of the continual effects of SAID convection channel crossing into the plasmasphere. As time goes on, the outer density peak of the troughs will be eroded by equatorial plasma convection, as is shown in Figures 11 and 12. When the LIFE of SAID is 60 min, two troughs aer formed, as shown in Figure 11(d), this phenomenal needs further investigation.

5 Summary and conclusion

566 SAID events observed by four satellites are identified to perform statistical analysis. The relationships between SAID signatures and certain geomagnetic indices such as Kp, Dst, and AL are analyzed. It is found that SAID events occur most probably between 55° and 66° ILAT and between 1930 and 2330 MLT, and occur mostly during medium geomagnetic activities, which is in good agreement with earlier studies [3, 19, 28]. The ILATC of SAID is fitted

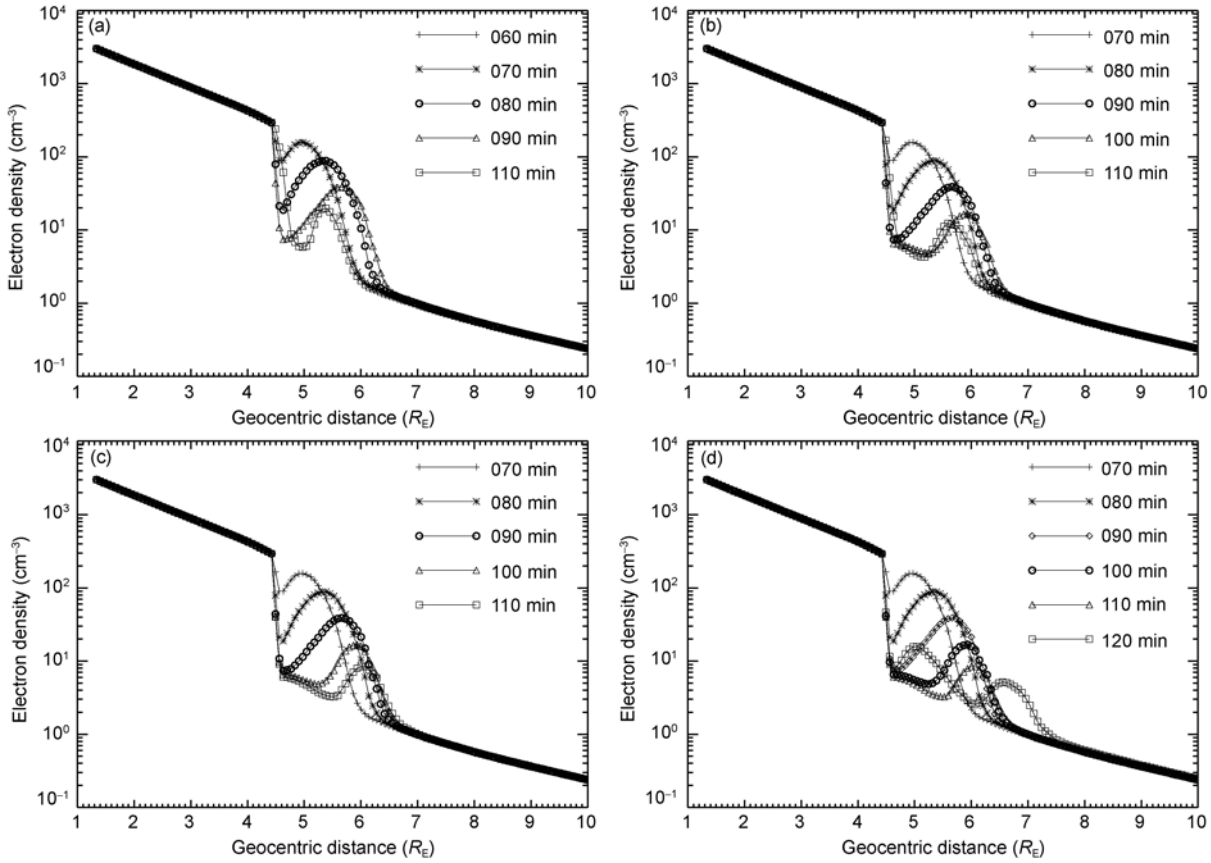

Figure 11 Equatorial plasmaspheric trough density profiles versus geocentric distance under different lifetimes of SAID events taken from the dusk sector in the simulations. From (a) to (d) the LIFEs of SAID are 30, 40, 50 and 60 min, respectively.

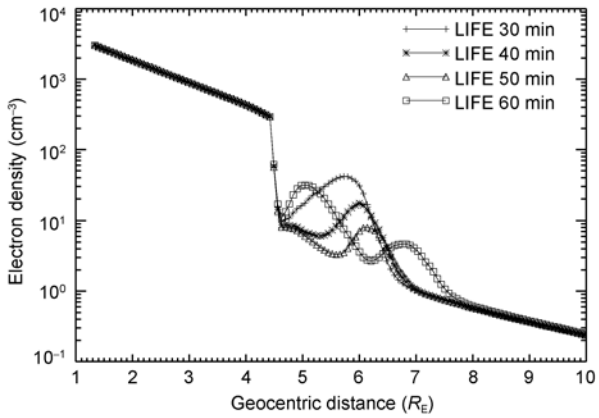

Figure 12 Trough density profiles versus geocentric distance after different LIFEs of SAID events.

to Kp, Dst, and AL indices. It reveals that the ILATC of SAID changes with these indices approximately exponentially. The IMF and solar wind dependence of SAID should be studied in future. We will combine other satellite data (such as DMSP satellites) to set up a more comprehensive SAID potential distribution model to investigate its effect on plasmaspheric trough in the future.

Using our statistical results and earlier models, the SAID effects on the equatorial plasmaspheric trough evolution in dusk and evening sector are simulated with DGCPM systematically. It is found that the locations, shapes and density of trough vary with ILATC, LATW, LONGC, CPCP, and LIFE of SAID events. The penetration of SAID electric field into plasmasphere changes with different locations and shapes of SAID, thus having different effects on trough formation and evolution. The trough is more apparent when the SAID potential is located between 60° and 61° ILAT, 1800 and 2100 MLT, with a latitudinal width of 1° to 2°. The radial width of trough increases quickly with the CPCP of the SAID. Different lifetime of SAID also results in different shape of trough and the trough tends to be deepened as time goes on. The existence of mid-latitude ionospheric density trough results in the erosion of flux tube, and the effect of equatorial convection continually erodes the plasmaspheric trough. However, the simple ionosphere potential and magnetic field model in our simulations can not exactly exhibit the dynamics of the ionosphere-plasmasphere coupling, and further improvements are needed in future works.

The main goal of this study is to improve our understanding on SAID signatures and their effects on outer plasmaspheric trough evolution. Further study will be nec-

essary to set up a new SAID potential model and to update the ionosphere convection model and the magnetic field model in DGCPM to study the formation and evolution of the trough in future. Simultaneous observations of SAID and plasmaspheric trough density will be used to study the effects of SAID on plasmasphere in future.

This work was supported by the National Natural Science Foundation of China (Grant Nos. 40890160, 40804030, 10878004, and 40974093), the National Basic Research Program of China ("973" Program) (Grant No. 2011CB811400, 2012CB957800), the National Hi-Tech Research and Development Program of China ("863" Program) (Grant No. 2010AA-122205), and the Special Fund for Public Welfare Industry (Grant Nos. GYHY200806024 and GYHY200906013). DE-2 IDM data used in this study are downloaded from NSSDC (NASA Space Science Data Center, http://nssdcftp.gsfc.nasa.gov/). The Akebono data are provided by Dr. A. MATSUOKA at Institute of Space and Astronautical Science (ISAS). The Freja data are provided by Dr. T. KARLSSON in Royal Institute of Technology (KTH) in Sweden. The Astrid-2 data are downloaded from the Alfvén Laboratory at http://www.spp.ee.kth.se/res/tools/astrid-2. All the geomagnetic indices are obtained from Kyoto World Data Center for Geomagnetism at http://swdcwww.kugi.kyoto-u.ac.jp/index.html.

1 Galperin Y I, Ponomarov Y N, Zosinova A G. Direct measurements of ion drift velocity in the upper atmosphere during a magnetic storm. Kosm Issled, 1973, 11(2): 273–282
2 Spiro R W, Heelis R H, Hanson W B. Rapid subauroral ion drifts observed by Atmospheric Explorer C. Geophys Res Lett, 1979, 6(8): 657–660
3 Anderson P C, Heelis R A, Hanson W B. The ionosphere signatures of rapid subauroral ion drifts. J Geophys Res, 1991, 96(A4): 5785–5792
4 Anderson P C, Hanson W B, Heelis R A, et al. A proposed production model of rapid subauroral ion drifts and their relationship to substorm evolution. J Geophys Res, 1993, 98(A4): 6069–6078
5 Anderson P C, Carpenter D L, Tsuruda K, et al. Multisatellite observations of rapid subauroral ion drifts (SAID). J Geophys Res, 2001, 106(A12): 29585–29599
6 Khalipov V L, Galperin Yu I, Stepanov A E, et al. Formation of polarization jet during injection of ions into the inner magnetosphere. Adv Space Res, 2003, 31(5): 1303–1308
7 Southwood D J, Wolf R A. An assessment of the role of precipitation in the magnetospheric convection. J Geophys Res, 1978, 83(A11): 5227–5232
8 Deminov M G, Shubin V N. Dynamics of the subauroral ionosphere under disturbance conditions. Geomagn Aeron Engl Transl, 1987, 27(3): 398–403
9 De Keyser J D, Roth M, Lemaire J. The magnetospheric driver of subauroral ion drift. Geophys Res Lett, 1998, 25(10): 1625–1628
10 De Keyser J D. Formation and evolution of subauroral ion drifts in the course of a substorm. J Geophys Res, 1999, 104(A6): 12339–12349
11 Galperin Y I. Polarization jet: Characteristics and a model. Ann Geophys, 2002, 20(3): 391–404
12 Ober D M, Horwitz J L, Gallagher D L. Formation of density troughs embedded in the outer plasmasphere by subauroral ion drift events. J Geophys Res, 1997, 102(A7): 14595–14602
13 Heelis R A, Hanson W B, Lippincott C R, et al. The ion drift meter for Dynamics Explorer-B. Space Sci Instrum, 1981, 5(12): 511–521
14 Hanson W B, Heelis R A, Power R A, et al. The retarding potential analyzer for Dynamics Explorer-B. Space Sci Instrum, 1981, 5(12): 503–510
15 Hayakawa H, Kohno Y I, Okada T, et al. Electric field measurement on the Akebono (EXOS D) satellite. J Geomagn Geoelectr, 1990, 42(4): 371–384
16 Marklund G T, Haerendel L G, Pederson A, et al. The double probe electric field experiment on Freja: Experiment description and first results. Space Sci Rev, 1994, 70(3-4): 483–508
17 Blomberg L G, Marklund G T, Lindqvist P-A, et al. Astrid-2: An advanced auroral microprobe. In: Hsiao F B, ed. Microsatellites as Research Tools. COSPAR Colloquia Series. Amsterdam: Elsevier, 1999, 10. 57–65
18 Tsyganeko N A. A magnetospheric magnetic field model with a wrapped tail current sheet. Planet Space Sci, 1989, 37(1): 5–50
19 Karlsson T, Marklund G T, Blomberg L G. Subauroral electric fields observed by the Freja satellite: A statistical study. J Geophys Res, 1998, 103(A3): 4327–4341
20 Feldstein Y I, Starkov G V. Dynamics of auroral belt and polar geomagnetic disturbances. Planet Space Sci, 1967, 15(2): 209–229
21 Hardy D A, Gussenhoven M S, Holeman E. A statistical model of auroral electron precipitation. J Geophys Res, 1985, 90(A5): 4229–4248
22 Hardy D A, Gussenhoven M S, Raistrick R, et al. Statistical and functional representations of the pattern of auroral energy flux, number flux, and conductivity. J Geophys Res, 1987, 92(A11): 12275– 12294
23 He F, Zhang X X, Chen B, et al. Calculation of the extreme ultraviolet radiation of the earth's plasmasphere. Sci China Tech Sci, 2010, 53(1): 200–205
24 Sojka J J, Rasmussen C E, Schunk R W. An interplanetary magnetic field dependent model of the ionospheric convection electric field. J Geophys Res, 1986, 91(A10): 11281–5232
25 Ober D M. The outer plasma as a source of magnetospheric plasmas, Doctoral Dissertation. Huntsville: University of Alabama, 1997
26 Horwitz J L, Comfort R H, Chappell C R. A statistical characterization of plasmasphere structure and boundary locations. J Geophys Res, 1990, 95(A6): 7937–7947
27 Burke W J, Rubin A G, Maynard N C, et al. Ionospheric disturbances observed by DMSP at middle to low-latitudes during magnetic storm of June 4-6, 1991. J Geophys Res, 2000, 105(A8): 18391–18405
28 Spiro R W, Heelis R A, Hanson W B. Ion convection and the formation of the mid-latitude F-region ionospheric trough. J Geophys Res, 1978, 83(A9): 4255–4264